Journal Pre-proof

Reduction of Chlorendic Acid by Zero-Valent Iron: Kinetics, Products, and Pathways

Min Sik Kim, Emily Piggott, Nick Zrinyi, Changha Lee, Anh Le-Tuan Pham

PII: S0304-3894(19)31223-3

DOI: https://doi.org/10.1016/j.jhazmat.2019.121269

Reference: HAZMAT 121269

To appear in: *Journal of Hazardous Materials*

Received Date: 7 August 2019

Revised Date: 8 September 2019

Accepted Date: 20 September 2019

Please cite this article as: Kim MS, Piggott E, Zrinyi N, Lee C, Le-Tuan Pham A, Reduction of Chlorendic Acid by Zero-Valent Iron: Kinetics, Products, and Pathways, *Journal of Hazardous Materials* (2019), doi: https://doi.org/10.1016/j.jhazmat.2019.121269

Reduction of Chlorendic Acid by Zero-Valent Iron: Kinetics, Products, and Pathways

*Min Sik Kim [1], Emily Piggott [2], Nick Zrinyi [2], Changha Lee [1], and Anh Le-Tuan Pham [3]**

[1] School of Chemical and Biological Engineering, Seoul National University, South Korea

[2] Department of Civil and Environmental Engineering, Carleton University
Ottawa, Ontario, Canada

[3] Department of Civil and Environmental Engineering, University of Waterloo
Waterloo, Ontario, Canada

(Manuscript prepared for submission to Journal of Hazardous Materials)

*Corresponding authors: Anh Le-Tuan Pham (email: anh.pham@uwaterloo.ca; phone: +1-519-888-4567 ext. 30337)

Highlights

- ZVI removed chlorendic acid (CA) from solution by adsorption and degradation
- The degradation of CA took place via stepwise reductive dechlorination reactions
- Ten products of CA transformation were detected, nine of which were identified
- The degradation of CA occurred under a wide range of water chemistry conditions
- ZVI is promising for the remediation of CA-contaminated groundwater

Abstract

Chlorendic acid (CA) is a recalcitrant groundwater contaminant for which an effective treatment technology does not currently exist. In this study, a series of batch experiments were conducted to investigate the treatment of CA by zero-valent iron (ZVI) under various water chemistry conditions. It was observed that CA was removed by ZVI via both adsorption and degradation, with the degradation rate being proportional to the fraction of CA adsorbed onto ZVI. The rate of CA degradation decreased as pH increased, presumably due to the passivation of ZVI and diminishing CA adsorption. Chloride (Cl^-) did not appreciably affect CA adsorption and degradation, while sulfate (SO_4^{2-}) significantly inhibited both processes because SO_4^{2-} competed with CA for ZVI adsorptive sites. The rate of CA degradation was significantly accelerated by ZVI-associated Fe(II). Nine byproducts of CA transformation were identified by high-resolution mass spectrometry. The formation and subsequent degradation of these products revealed that the transformation of CA by ZVI occurred via a step-wise reductive dechlorination pathway. Overall, this study suggests that ZVI may be effective at remediating CA-contaminated sites.

Keywords: Chlorendic acid, zero-valent iron, reductive dechlorination, remediation, hazardous waste.

1. Introduction

Chlorendic acid (CA) is a polychlorinated organic compound used in the synthesis of polymeric resins, corrosion-resistant plastics, flame retardants, and other materials [1,2]. It is present at sites where CA-containing wastes were disposed [3,4]. CA is also a transformation byproduct of chlorinated norbonenes such as heptachlor [5]. Similar to many polychlorinated compounds (e.g.,

polychlorinated biphenyls, hexachloro norbonene pesticides and flame retardants), CA is highly resistant to biological transformation [3,6]. Unlike most polychlorinated compounds, however, CA has a relatively high aqueous solubility (C_w^s = 3.5 g/L, [2]) and therefore is more likely to be an aqueous contaminant rather than a soil or sediment contaminant. At contaminated sites, the potentially high mobility of CA together with its persistence may present significant challenges to efforts at containing and mitigating CA plumes.

To identify potential technologies for the remediation of CA, in our previous study we examined the ability of activated persulfates to destroy CA [7]. In an experiment involving a mixture of groundwater and aquifer soils, we observed a rapid loss of CA following persulfate amendments. However, this loss was not the result of oxidative transformation. Rather, the loss was attributable to the adsorption of CA on aquifer soils due to the acidification of the solution as persulfate decomposed. The adsorption of CA prevented it from reacting with sulfate ($SO_4^{\bullet-}$) and hydroxyl ($^{\bullet}OH$) radicals. As such, once all persulfate was consumed and the pH of the solution increased to the pre-treatment level, CA desorbed from the aquifer soils and the concentration of CA rebounded to the baseline concentration. We also observed that the affinity of CA to aquifer soils and to various types of solids (SiO_2, Fe-oxyhydroxide, MnO_2) was strongly dependent on the solution pH, with more CA adsorbing to the solids under acidic conditions than under neutral and alkaline conditions. This finding suggests that the fate and transport of CA can be influenced by the geology and water chemistry condition of the contaminated site. Finally, while previous studies indicated that $^{\bullet}OH$ and $SO_4^{\bullet-}$ were capable of oxidizing CA [8–10], we found that CA was only moderately reactive with these radicals ($k_{\bullet OH}$ = (8.71 ± 0.17) × 10^7 M^{-1} s^{-1} and $k_{SO4\bullet-}$, = (6.57 ± 0.83) × 10^7 M^{-1} s^{-1} at 24.5 °C for the reaction with $^{\bullet}OH$ and $SO_4^{\bullet-}$, respectively) [7]. This means that even under conditions in which CA does not adsorb to solids, the transformation of CA by $^{\bullet}OH$ and $SO_4^{\bullet-}$ is

not expected to occur appreciably if radical scavengers such as natural organic matter, bicarbonate, and co-contaminants are present. Collectively, our findings suggest that the oxidation of CA by activated persulfates or by other radical-based treatments (e.g., Fenton's reaction) may occur only under certain specific conditions.

For the remediation of CA, an alternative approach to oxidation could be reacting CA with a strong reductant such as zero-valent iron (ZVI). ZVI is used in permeable reactive barriers (PRB) or is injected into the subsurface to treat groundwater contaminated with chlorinated solvents such as perchloroethylene (PCE), trichloroethylene (TCE), carbon tetrachloride (CT), as well as other contaminants [11–14]. ZVI can potentially be effective at destroying CA considering that CA has structural features similar to those of chlorinated solvents (i.e., carbon-chlorine bonds, carbon-carbon double bond). While the tendency of CA to associate with surfaces is undesirable in $^{\bullet}OH$ and $SO_4^{\bullet-}$-based treatment systems (since these radicals only react with aqueous-phase solutes), adsorption of CA to ZVI can be beneficial as adsorption is one of the key steps in the reaction between contaminants and ZVI [14]. Also, unlike in the persulfate-based treatment systems, the pH of the solution in the ZVI-based systems often remains in the circumneutral range. Therefore, CA will have lower tendency to adsorb to aquifer soils and thus will be more available to react with ZVI.

To test the above hypotheses and to assess the potential of ZVI for CA remediation, a series of experiments were conducted to investigate the reaction between ZVI and CA, the formation of products, the role of adsorption on the reaction rate, and the influence of water chemistry parameters such as solution pH, chloride (Cl^-), sulfate (SO_4^{2-}), and dissolved iron(II) (Fe(II)). In each experiment, the amounts of CA in the solution and adsorbed on ZVI were carefully quantified to differentiate between the CA loss by adsorption and by transformation. Additionally, the

products of CA degradation were identified using high-resolution mass spectrometry to establish the pathway of transformation.

2. Materials and methods

2.1 Chemicals.

All chemicals were of reagent grade and were used without further purification. ZVI powder (5–9 μm) was purchased from STREM Chemicals. Acetonitrile was purchased from Honeywell. Aqueous solution of 0.1% v/v formic acid was purchased from Thermo Fisher Scientific. The other chemicals, including chlorendic acid (CA), 2-(*N*-morpholino)ethanesulfonic acid (MES), 1,4-piperazinediethanesulfonic acid (PIPES), 1,10-phenathroline, acetic acid (CH_3COOH), sodium acetate (CH_3COONa), ammonium acetate (CH_3COONH_4), hydroxylamine (NH_2OH), iron(II) chloride tetrahydrate ($FeCl_2 \bullet 4H_2O$), sodium chloride (NaCl), sodium sulfate (Na_2SO_4), phosphoric acid (H_3PO_4), hydrochloric acid (HCl), perchloric acid ($HClO_4$), and sodium hydroxide (NaOH) were purchased from Sigma-Aldrich. All solutions were prepared using deionized water (> 18.2 MΩ cm, Millipore).

2.2 Experimental setup and procedures.

All experiments were carried out under anoxic condition at room temperature (22 ± 1°C). The reaction solutions usually consisted of 0.1 mM CA, 0–10 mM of either NaCl or Na_2SO_4, and 5 mM of either MES, PIPES, or acetate which served as a pH buffer. The concentration of CA used in this study was similar to those employed by others [8–10], and was representative of the CA concentrations that could be found at CA-impacted sites [3, 4]. The pH of each solution was adjusted to a desired value by either 1 M NaOH or 1 M $HClO_4$. For the solutions that were buffered with MES or PIPES, throughout the course of the experiment the pH remained in the range of 5.8 – 7.3 and 6.3 – 7.3, respectively. For the solutions that were buffered by acetate, the initial pH was

adjusted to 3.5 – 5, but the pH always rose quickly to pH 5.5 – 6.5. After pH adjustment, the solution was purged with ultrapure N_2 gas, transferred into a N_2-filled glove box, and the concentration of dissolved oxygen in the solution was measured by a dissolved oxygen probe to ensure that $[O_2]_{dissolved}$ was less than 0.2 mg/L. Within the glove box, aliquots of 10 mL of the solution were transferred into 15-mL test tubes which contained 5 g ZVI, resulting in a ZVI concentration of 500 g/L in each reaction solution. (This high concentration of ZVI was chosen to accelerate the transformation of CA's byproducts, allowing us to investigate the formation and subsequent degradation of each product in a reasonable experimental timescale). Subsequently, the test tubes were carefully sealed and placed on an end-over-end rotator. At predetermined time intervals, two to three test tubes were taken off from the rotator and were placed on a rack for 30 s to allow the ZVI particles to settle; essentially all ZVI settled to the bottom after 30 s. Subsequently, 8 mL of the supernatant was taken out, filtered through a 0.45-μm syringe filter, and the filtrate was analyzed for pH, CA, and transformation products (in some experiments). To account for the fraction of CA that was lost due to adsorption on ZVI, 5 mL of 0.05 M NaOH was added to the remaining ZVI suspension in the test tube, and the tube was vigorously mixed for 3 min. An aliquot was then subsampled, filtered, and analyzed for CA. Our previous study has shown that this extraction procedure can recover more than 90% of the CA adsorbed on mineral surfaces [7]. Therefore, the fraction of CA that was lost due to transformation by ZVI, $[CA]_{transformed}$, can be calculated by the following mass balance equation:

$$[CA]_{transformed} = [CA]_0 - [CA]_t - [CA]_{adsorbed,\ t}$$

with $[CA]_0$, $[CA]_t$, and $[CA]_{adsorbed,\ t}$ being the initial CA, the CA remained in the solution, and the CA adsorbed on ZVI, respectively.

Two separate sets of experiments were conducted to examine the effects of dissolved Fe(II) on the kinetics of CA transformation. In the first set of experiments, the reaction solution was prepared as described above, but prior to transferring into the ZVI-containing test tubes the solution was amended with 50 or 200 μM $FeCl_2$. In the second set of experiments, the de-aerated solution initially did not contain any CA. This solution was amended with 50 or 200 μM $FeCl_2$, and 10 mL aliquots were transferred to ZVI-containing test tubes. After an equilibration time of 30 min to allow some Fe(II) to adsorb on ZVI, CA was added to the test tubes to initiate transformation reactions. At pre-determined time intervals, the fractions of CA in the solution and on ZVI were quantified following the procedure described above. The total dissolved Fe (i.e., dissolved Fe(II) and Fe(III)) in the solution was also quantified. The average solution pH throughout the course of these experiments was pH_{ave} = 6.2, and although no pH buffer was used, the solution pH varied by less than ± 0.5 pH unit.

One more set of experiments was conducted to investigate the effect of pH on the adsorption of CA on ZVI. In this set of experiments, the solution pH was adjusted to a desired value inside the glove box (no pH buffer was used), and 10 mL aliquots were transferred into ZVI-containing test tubes. After a very short mixing time (less than 30 s), an aliquot was taken out, filtered, and analyzed for CA and pH. Although adsorption equilibrium is unlikely to have been attained within 30 s, the objective of this experiment was simply to assess the affinity of CA to ZVI surface as well as to investigate how this affinity changed under different water chemistry conditions.

2.3 Analytical Methods.

The surface area of ZVI was determined using the 5 point BET (Brunauer-Emmett-Teller) N_2 physisorption method. Total dissolved Fe was measured using the 1,10-phenanthroline method

after acidification and reduction of Fe(III) with NH_2OH•HCl [15]. CA was measured using a rapid separation liquid chromatography (RSLC) (Ultimate 3000, Dionex) with UV absorbance detection at 225 nm. The chromatographic separation was performed on an AcclaimTM C18 column (2.1 mm × 150 mm, 2.2 μm, 120 Å; Thermo Fisher Scientific) using 50:50 mixture of 0.1 wt. % phosphoric acid and neat acetonitrile as eluent at a flow rate of 0.3 mL/min. The concentration of CA in each sample was determined from a concentration-UV absorbance calibration curve that was established based on standard solutions of varying CA concentration. The transformation products of CA were analyzed by RSLC coupled with Q-Exactive Hybrid Quadrupole-Orbitrap mass spectrometry (Thermo Fisher Scientific) (LC/MS). The chromatographic separation conditions were the same as above except that 0.1 wt. % formic acid was used instead of phosphoric acid. The heated electrospray ionization (ESI) source interface was operated in the negative ionization mode under the following conditions: spray voltage was 3.5 kV, sheath gas was 40 arbitrary units, auxiliary gas was 10 arbitrary units, no sweep gas, capillary and vaporized temperature were 320˚C and 350˚C, respectively. Mass spectra were obtained in full scanning mode from 100 to 500 m/z at a resolution of 35,000. To achieve high mass accuracy, LC/MS calibration was performed before the analysis using a Pierce^{TM} ESI negative ion calibration solution. Data acquisition and processing were performed using Xcalibur 3.0.2 software (Thermo Fisher Scientific). The mass spectra of CA and the products contained multiple $[M\text{-}H]^-$ isotopic peaks, which is typical for compounds consisting of Cl and O atoms. In this study, the evolution of each compound was examined by monitoring the peak of lowest $[M\text{-}H]^-$ mass value. Since the standards for the products were not available, the evolution of each product over time was qualitatively assessed based on the chromatographic peak area.

3. Results and discussion

3.1 Pathway and products of CA transformation

In the presence of ZVI, CA was removed from the solution by both adsorption and transformation (Fig. 1). Unlike in the persulfate systems in which the association of CA with mineral surfaces prevented CA from reacting with $^{\bullet}OH$ and $SO_4^{\bullet-}$ [7], the adsorption of CA by ZVI did not appear to inhibit CA transformation. At t = 4h, nearly all of the CA remained in the system (~ 50%) was associated with the surface of ZVI, yet the transformation reaction continued (Fig. 1). This is consistent with the consensus agreement on the mechanism through which contaminants are reduced by ZVI, that is the contaminant must first adsorb on ZVI before the transformation step can occur [12,14]. After 6 hours, approximately 70% of CA was removed by transformation, while the other 30% was removed by adsorption.

To further assess the ability of ZVI to destroy CA, the evolution of transformation products was monitored in an experiment that spanned over 6 weeks (Fig. 2). Under the conditions of this experiment, the reaction between CA and ZVI produced 10 different products whose nominal $[M-H]^-$ masses rounded to the nearest whole number were 351, 317, 301, 299, 283, 267, 249, 233, 215, and 181 Da (denoted from this point forward as products P351, P317, P301 etc.). Based on the $[M-H]^-$ exact masses (Table S1), we were able to identify the molecular formula for all except one product (Scheme 1 and Table S1). The masses of CA and products P351, P317, P283, P249, P215, P181 differed by $\Delta m = 33.961$ Da, which is the mass change that would have been resulted from replacing a Cl atom by a H atom. As such, the transformation of CA is proposed to have occurred via sequential reductive dechlorination reactions that ultimately generated P181, the product which did not contain any Cl atom (reactions *1-6* in Scheme 1). The peak area-time profiles of each product reveal that the products were generated and subsequently degraded, with the

exception of P233 (Fig. 2). The general trend was that the products containing more Cl atoms were more reactive with ZVI: P351 disappeared at a faster rate than did P317, and P317 in turn disappeared at a faster rate than did the other products. A similar trend in reactivity with ZVI was observed for CCl_4 and its transformation products [11]. P181 appeared to be further degraded (Fig. 2b), but the product(s) of this degradation could not be detected using the described LC/MS method.

The mass difference between P317 and P299 was $\Delta m = 17.966$ Da, which suggests that P299 was generated via the hydrolysis of P317 (reaction *7*). However, the transformation of P317 via this pathway is likely less important than via reaction *3* because the transformation of chlorinated compounds by neutral hydrolysis is generally slow under room temperature [16]. P301 is proposed to be formed via the hydrogenation of the double bond in P299 (reaction *8*). P301 was subsequently transformed into P267 by reductive dechlorination (reaction *9*; the mass difference between P301 and P267 was also $\Delta m = 33.961$ Da).

A reasonable molecular formula for P233 and the pathway through which it was generated could not be determined. P233 was not formed from the reductive dechlorination of P267 because the mass difference between the two compounds was $\Delta m = 33.865$ Da, which is significantly different from $\Delta m = 33.961$ Da. Interestingly, P233 appeared to be more hydrophobic than the other products, including those that have higher molecular weight (e.g., P351), because its retention time in the C_{18} column was the greatest among the products (Fig. S1). Unlike the other products, P233 was not further degraded within the timeframe of this experiment (Fig. 2).

3.2 Effects of solution chemistry on CA adsorption and transformation rate

The results presented in the previous section showed that ZVI was effective at destroying both CA and its products. To further assess the utility of ZVI for CA remediation, the reaction between CA

and ZVI was studied under various solution conditions to examine the effects of pH, Cl^-, SO_4^{2-}, and dissolved Fe(II) on the adsorption and transformation of CA, as well as to explore the trend between these two removal mechanisms.

CA adsorption. The adsorption of CA seen in Fig. 1 could be attributable specifically to the adsorption by the iron (hydr)oxide layer on the surface of ZVI. The ZVI in this study was a commercial product and was used without any further treatment. Therefore, it is likely that its surface was already partially oxidized prior to the experiments. Previous studies have shown that CA had some affinity to iron hydroxides [4,7]. In the current study, the affinity of CA to ZVI was further investigated by employing an experiment in which the reaction solution was in contact with ZVI particles for less than 30 s. (The transformation of CA during this very short contact time is expected to be minimal – refer to SI for further explanation). This experiment revealed that the adsorption of CA on ZVI was strongly affected by the solution pH, with more CA adsorbed at acidic pH than at neutral pH (Fig. 3). This trend, which was similar to those observed in the CA-metal oxide systems [7], suggests that CA adsorption could have been driven by electrostatic interactions. The point of zero charge (pzc) of iron (hydr)oxides typically ranges from 7.5 to 9 [17]. Therefore, the surface of ZVI would have become more positively charged as pH decreased from 9 to 2, and would have exerted an increasingly stronger attraction force on the negatively charged CA molecules (CA has a pK_{a1} = 3.1 and a pK_{a2} = 4.6 [6]).

CA adsorption also appeared to be controlled by the type of electrolyte present in the solution. The presence of 10 mM Cl^- did not appreciably affect CA adsorption at pH < 6, and only slightly diminished the adsorption at pH > 6 (Fig. 3). In contrast, 10 mM SO_4^{2-} significantly decreased the CA adsorption at all pH values. A possible explanation for the effect of Cl^- and SO_4^{2-} could be that these anions were competing with CA for adsorptive sites. The stronger effect of the SO_4^{2-}

anions might be attributable to their ability to form inner-sphere complexes with the iron (hydr)oxide layer on the surface of ZVI [18,19]. An alternative explanation could be that the corrosion layers formed on the ZVI surface in the presence of Cl^- and SO_4^{2-} might have lower adsorption affinity for CA. However, this explanation is less likely considering the very short contact time between the reaction solution and ZVI in this experiment. Finally, although cannot be entirely excluded, the greater ionic strength of the 10 mM Na_2SO_4 solution than that of the 10 mM NaCl solution (ΔI between the two solutions was around 20 mM) was unlikely the reason why less CA was adsorbed in the 10 mM Na_2SO_4 solution. As will be seen in the next section, the fraction of CA adsorbed on ZVI remained relatively unchanged when the concentration of Cl^- was varied.

CA transformation rate. The pseudo-first order reductive dechlorination rate constant, k_{red}, for the reaction between CA and ZVI can be obtained from the plot of ln $[CA]_{transformed}/[CA]_0$ *versus* time (insets of Fig. 1 and Fig. S2). The pH – k_{red} trend is presented in Fig. 4, revealing that k_{red} progressively decreased as pH increased. Possible explanations for the slower CA transformation rate at higher pH include lower adsorption of CA (Fig. 4) and/or passivation of ZVI. As mentioned earlier, the adsorption of contaminant on ZVI is prerequisite for the reduction of the contaminant, whereas the ZVI's decreased reactivity at higher pH can be caused by passivation [11,20,21]. Alternatively, if H^+ were to be directly involved in the rate-limiting step of the reductive transformation reaction, a decrease in $[H^+]$ also would have resulted in a slower transformation rate. However, this explanation is less likely since the slope of the pH – log ($1/ k_{red}$) plot was 0.18 (Fig. S3), which is significantly smaller than 1 (i.e., the slope value indicative of the involvement of H^+ in the rate limiting step).

Cl^- and SO_4^{2-} are among the common solutes present in groundwater, and Cl^- is also a byproduct of the reductive dechlorination of CA. Numerous studies have shown that the reduction of contaminants by ZVI was faster in the presence of Cl^- and SO_4^{2-} [21–27]. However, there are also studies reporting that Cl^- and SO_4^{2-} slowed contaminant transformation [13,28,29]. The positive effect of Cl^- and SO_4^{2-} was attributable to the ability of these anions at destroying the passivation layer, thereby regenerating reactive sites on the ZVI surface. In contrast, the negative effect of Cl^- and SO_4^{2-} was thought to be caused by fewer available reactive site due to the adsorption of these anions on ZVI. It appears that whether Cl^- and SO_4^{2-} accelerate or decelerate the transformation of contaminants depends on the surface state of ZVI (e.g., freshly synthesized vs. aged ZVI), the type of contaminant and its concentration, the concentrations of Cl^- and SO_4^{2-}, and other factors. In our study, Cl^- had a mixed effect on the CA transformation rate. Specifically, the presence of Cl^- slightly slowed the CA degradation at pH 6.3, and accelerated the degradation at pH 7.6 (Fig. 5a, Fig. S4 and S5). However, k_{red} remained unchanged when the concentration of Cl^- varied from 1 to 10 mM, and neither the presence nor the concentration of Cl^- appreciably affected the adsorption of CA. Therefore, the competitive adsorption between Cl^- and CA could not be invoked to explain the effect of Cl^- on k_{red}. Rather, the faster CA transformation at pH 7.6 could be due to the ability of Cl^- to prevent ZVI passivation. However, the reason why Cl^- slowed the transformation at pH 6.3 is unclear.

Different from Cl^-, the presence of SO_4^{2-} always retarded the transformation of CA, and the concentration of SO_4^{2-} was inversely proportional to the fraction of CA adsorbed and the transformation rate (Fig. 5b). These trends suggest that the effect of SO_4^{2-} on the rate of CA transformation could be attributable, at least in part, to the diminished CA adsorption. However, it was also observed that k_{red} at pH 6.3 was 2 to 2.5 times higher than that at pH 7.6 even though a

similar amount of CA was adsorbed (e.g., when $[SO_4^{2-}]$ = 1 mM, the fractions of CA adsorbed were 8% under both pH regimes, but k_{red} were 0.026 h^{-1} and 0.06 h^{-1} at pH 7.6 and 6.3, respectively). As such, the slower CA degradation at pH 7.6 might be related to the more pronounced ZVI passivation at this pH value.

As with Cl^- and SO_4^{2-}, dissolved Fe(II) has been observed to accelerate the rate of contaminant transformation by ZVI in some studies [30–32], while retarding the transformation in another [27]. The positive effect of Fe(II) was attributed to the surface-associated Fe(II) facilitating electron transfer from ZVI to the contaminant, while the inhibitory effect of Fe(II) was thought to be caused by the precipitation of Fe(II) which passivated ZVI and decreased the reactivity of the latter. In our experiments, depending on how dissolved Fe(II) was added to the test solution, Fe(II) either had no appreciable effect or accelerated the transformation of CA (Fig. 5c and Fig. S6). Specifically, in the experiment in which dissolved Fe(II) was not pre-equilibrated with ZVI, the average k_{red} value was 0.18–0.19 h^{-1}, which was only slightly higher than those measured in the experiments in which no additional dissolved Fe(II) was supplemented (Fig. 4, k_{red} measured at a similar pH, 6.2, ranged from 0.13–018 h^{-1}). In contrast, in the experiment in which the supplemented dissolved Fe(II) was pre-equilibrated with ZVI before CA was added, the average k_{red} value was 1.5 to 2 times greater, ranging from 0.28 to 0.31 h^{-1}. The fraction of CA adsorbed in these experiments was comparable to those in the experiments conducted at a similar pH value, suggesting that the faster CA transformation was not due to greater CA adsorption. Rather, the faster transformation might have been due to the reaction between CA and the ZVI-associated Fe(II). Measurement of the dissolved Fe(II) in the reaction solution corroborates this hypothesis, because approximately 12–30% of the added Fe(II) was associated with ZVI prior to the addition of CA, and throughout the course of the experiment the amount of dissolved Fe in this experiment

was generally lower than that in the experiment in which Fe(II) was not pre-equilibrated with CA (Fig. S7).

Trend between CA adsorption and transformation. The results presented above showed that the fraction of CA adsorbed on ZVI was correlated with k_{red} under some conditions, while was not in some other conditions. To gain a better picture of the trend between these two parameters as well as to compare k_{red} values among the experiments, all the k_{red} and $[CA]_{adsorbed}$ values obtained in this study were replotted in Fig. 6. As seen from this figure, with the exception of the Fe(II)-associated ZVI system, there was generally a good correlation between $[CA]_{adsorbed}$ and k_{red}, with faster CA transformation observed under conditions that were more favorable for CA adsorption. It can also be seen that Cl^- did not have a discernable effect on the transformation rate, while SO_4^{2-} decelerated the transformation. Lastly, as discussed earlier, the rate of CA transformation was substantially higher in the system containing Fe(II)-associated ZVI.

Surface area-normalized transformation rate constant. In addition to being controlled by the solution chemistry, the contaminant transformation rate in by ZVI is also controlled by the ZVI concentration and the type of ZVI. To be able to compare of the reactivity of CA with ZVI to those of other chlorinated organic solvents, the k_{red} values obtained in this study (0.026–0.31 h^{-1}) were normalized by the surface area of the ZVI (0.3 m^2/g) to obtain the surface-area normalized pseudo-first order reaction rate constant, $k_{red\text{-}surf}$. In this study, $k_{red\text{-}surf}$ ranged between 2×10^{-4} and 2×10^{-3} L h^{-1} m^{-2}, which was similar to the $k_{red\text{-}surf}$ values ($k_{red\text{-}surf} = 6 \times 10^{-5}$–$10^{-3}$ L h^{-1} m^{-2}) for TCE reported in different studies (Fig. 6 in [33]). This analysis suggests that the reactivity of CA with ZVI is comparable to that of TCE, and that like TCE, CA may be remediated in situ by ZVI permeable reactive barriers, or by the injection of nanoparticulate ZVI into the subsurface.

4. Conclusions

This study investigated the treatment of chlorendic acid by zero-valent iron. Key findings are summarized below:

- ZVI removed CA from the solution by both adsorption and transformation. Unlike in the oxidative treatment system [7], the adsorption of CA onto ZVI did not inhibit the transformation. Rather, the adsorption appeared to accelerate the transformation under most conditions.
- The fraction of CA adsorbed on ZVI and the transformation rate increased as the solution pH decreased. The transformation of CA was also accelerated by ZVI-associated Fe(II).
- Chloride did not appreciably affect CA adsorption and transformation, while sulfate significantly diminished both processes. The effect of sulfate was attributable to its ability to compete with CA for ZVI adsorptive sites.
- The reactivity of CA with ZVI was comparable to that of TCE, suggesting that treatment of CA by ZVI can be an effective method for the remediation of CA-contaminated sites.
- The transformation of CA by ZVI took place via sequential reductive dechlorination reactions. Ten products were detected in this study, nine of which were identified. The identified products were degraded further by ZVI. Future research is needed to identify all byproducts and to investigate their toxicity.

Acknowledgement. Funding for this research was provided by Ontario Centres of Excellence (VIP1 Grant #27828), and Natural Sciences and Engineering Research Council of Canada (Discovery Grant #2015-04850).

Supporting information: Fig. S1-S7

References

1. NTP. NTP toxicology and carcinogenesis studies of chlorendic acid (CAS No. 115-28-6) in F344/N rats and B6C3F1 mice (feed studies). Natl. Toxicol. Program Tech. Rep. Ser. 304, (1987) 1–225.
2. IPCS, 1996. Chlorendic acid and anhydride. World Health Organization.
3. W.-C. Ying, R.R. Bonk, V.J., Lloyd, S.A. Sojka, Biological treatment of a landfill leachate in sequencing batch reactors. Environ. Prog. 5 (1986) 41–50.
4. W.-C. Ying, J.J. Duffy, M.E. Tucker, Removal of humic acid and toxic organic compounds by iron precipitation. Environ. Prog. 7 (1988) 262–269.
5. W.P. Cochrane, M.A. Forbes, Oxidation products of heptachlor and its metabolites – A chemical study. Chemosphere 3 (1974) 41–46.
6. P.F. Hendrix, J.A. Hamala, C.L. Langner, H.P. Kollig, Effects of chlorendic acid, a priority toxic substance, on laboratory aquatic ecosystems. Chemosphere 12 (1983) 1083–1099.
7. A. Taylor, N. Zrinyi, S.P. Mezyk, J.M. Gleason, L. MacKinnon, A. Przepiora, A.L.-T. Pham, In-situ chemical oxidation of chlorendic acid by persulfate: Elucidation of the roles of adsorption and oxidation on chlorendic acid removal. Water Res. 162 (2019) 78–86.
8. J.P. Stowell, J.N. Jensen, Dechlorination of chlorendic acid with ozone. Water Res. 25 (1991) 83–90.

9. N. Boisa, Photo-catalytic degradation of chlorendic acid: 1. Degradation products. J. Appl. Sci. Environ. Manage. 17 (2013) 335–340.

10. N. Hermes, G. Knupp, Transformation of atrazine, bisphenol A and chlorendic acid by electrochemically produced oxidants using a lead dioxide electrode. Environ. Sci.: Water Res. Technol. 6 (2015) 905–912.

11. L.J. Matheson, P.G. Tratnyek, Reductive dehalogenation of chlorinated methanes by iron metal. Environ. Sci. Technol. 28 (1994) 2045–2053.

12. W.A. Arnold, A.L. Roberts, Pathways and kinetics of chlorinated ethylene and chlorinated acetylene reaction with Fe(0) particles. Environ. Sci. Technol. 34 (2000) 1794–1805.

13. Y. Liu, T. Phenrat, G.V. Lowry, Effect of TCE concentration and dissolved groundwater solutes on NZVI-promoted TCE dechlorination and H_2 evolution. Environ. Sci. Technol. 41 (2007) 7881–7887.

14. P.G. Tratnyek, M.M. Scherer, T.L. Johnson, L.J. Matheson, Permeable reactive barriers of iron and other zero-valent metals, in: M.A. Tarr (Ed.), Chemical Degradation Methods For Wastes And Pollutants: Environmental and Industrial Applications, Marcel Dekker Inc., New York, USA, 2003, pp. 371–421.

15. H. Tamura, K. Goto, T. Yotsuyanagi, M. Nagayama, Spectrophotometric determination of iron(II) with 1,10-phenanthroline in the presence of large amounts of iron(III). Talanta 21 (1974) 314–318.

16. P.M. Jeffers, L.M. Ward, L.M. Woytowitch, N.L. Wolfe, Homogeneous hydrolysis rate constants for selected chlorinated methanes, ethanes, ethenes, and propanes. Environ. Sci. Technol. 23 (1989) 965–969.

17. D.A. Sverjensky, N. Sahai, Theoretical prediction of single-site surface-protonation equilibrium constants for oxides and silicates in water. Geochim. Cosmochim. Acta 60 (1996) 3773–3797.

18. T. Sugimoto, Y. Wang, Mechanism of the shape and structure control of monodispersed α-Fe_2O_3 particles by sulfate ions. J. Colloid Interf. Sci. 207 (1998) 137–149.

19. C.M. Eggleston, S. Hug, W.S. Stumm, B. Sulzberger, M.D.S. Afonso, Surface complexation of sulfate by hematite surfaces: FTIR and STM observations. Geochim. Cosmochim. Acta 62 (1998) 585–593.

20. Z. Wang, P. Peng, W. Huang, Dechlorination of γ-hexachlorocyclohexane by zero-valent metallic iron. J. Hazard. Mater. 166 (2009) 992–997.

21. W. Yin, J. Wu, P. Li, X. Wang, N. Zhu, P. Wu, B. Yang, Experimental study of zero-valent iron induced nitrobenzene reduction in groundwater: The effects of pH, iron dosage, oxygen and common dissolved anions. Chem. Eng. J. 184 (2012) 198–204.

22. E. Lipczynska-kochany, S. Harms, R. Milburn, G. Sprah, N. Nadarajah, Degradation of carbon tetrachloride in the presence of iron and sulphur containing compounds. Chemosphere 29 (1994) 1477–1489.

23. T.L. Johnson, W. Fish, Y.A. Gorby, P.G. Tratnyek, Degradation of carbon tetrachloride by iron metal: Complexation effects on the oxide surface. J. Contam. Hydrol. 29 (1998) 379–398.

24. J.F. Devlin, K.O. Allin, Major anion effects on the kinetics and reactivity of granular iron in glass-encased magnet batch reactor experiments. Environ. Sci. Technol. 39 (2005) 1868–1874.

25. J.S. Kim, P.J. Shea, J.E. Yang, J.-E. Kim, Halide salts accelerate degradation of high explosives by zerovalent iron. Environm. Pollut. 147 (2007) 634–641.

26. E. Bi, L. Bowen, J.F. Devlin, Effect of mixed anions (HCO_3^-–SO_4^{2-}–ClO_4^-) on granular iron (Fe^0) reactivity. Environ. Sci. Technol. 43 (2009) 5975–5981.

27. Y.-F. Su, C.-Y. Hsu, Y.-H. Shih, Effects of various ions on the dechlorination kinetics of hexachlorobenzene by nanoscale zero-valent iron. Chemosphere 88 (2012) 1346–1352.

28. A.M. Moore, C.H. De Leon, T.H. Young, Rate and extent of aqueous perchlorate removal by iron surfaces. Environ. Sci. Technol. 37 (2003), 3189–3198.

29. Y. Hwang, D. Kim, H.-S. Shin, Inhibition of nitrate reduction by NaCl adsorption on a nano-zero-valent iron surface during a concentrate treatment for water reuse. Environ. Technol. 36 (2015) 1178–1187.

30. C. Tang, Y.H. Huang, H. Zeng, Z. Zhang, Reductive removal of selenite by zero-valent iron: The roles of aqueous Fe^{2+} and corrosion products, and selenate removal mechanisms. Water Res. 67 (2014) 166–174.

31. S. Bae, K. Hannah, Reactivity of nanoscale zero-valent iron in unbuffered systems: Effect of pH and Fe(II) dissolution. Environ. Sci. Technol. 49 (2015) 10536–10543.

32. L. Han, L. Yang, H. Wang, X. Hu, Z. Chen, C. Hu, Sustaining reactivity of Fe^0 for nitrate reduction via electron transfer between dissolved Fe^{2+} and surface iron oxides. J. Hazard. Mater. 308 (2016) 208–215.

33. T.L. Johnson, M.M. Scherer, P.G. Tratnyek, Kinetics of halogenated organic compound degradation by iron metal. Environ. Sci. Technol. 30 (1996) 2634–2640.

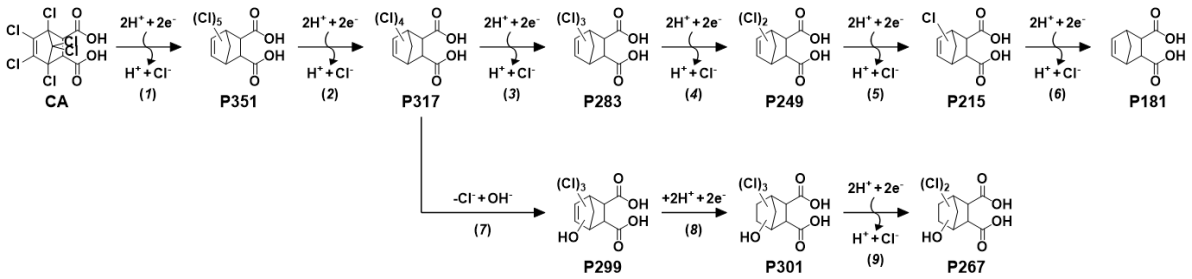

Scheme 1. Reductive transformation of CA by ZVI.

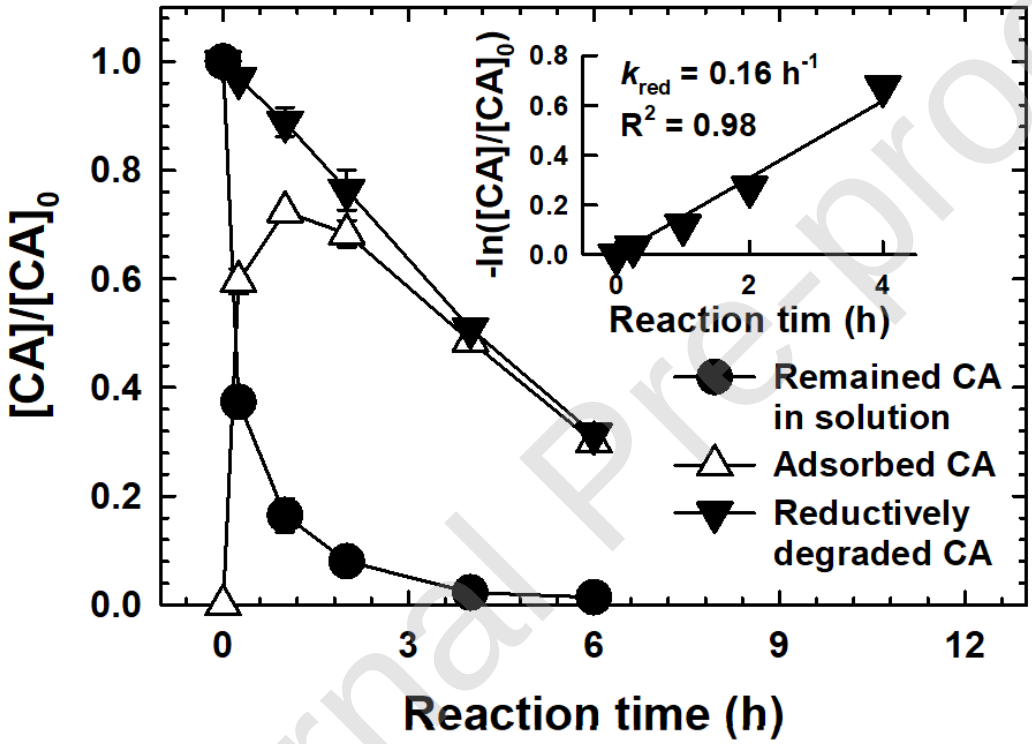

Fig. 1. Removal of CA by adsorption onto ZVI and reductive transformation. [ZVI] = 500 g/L, [MES] = 5 mM, $pH_{initial}$ = 7, pH_{ave} = 7.

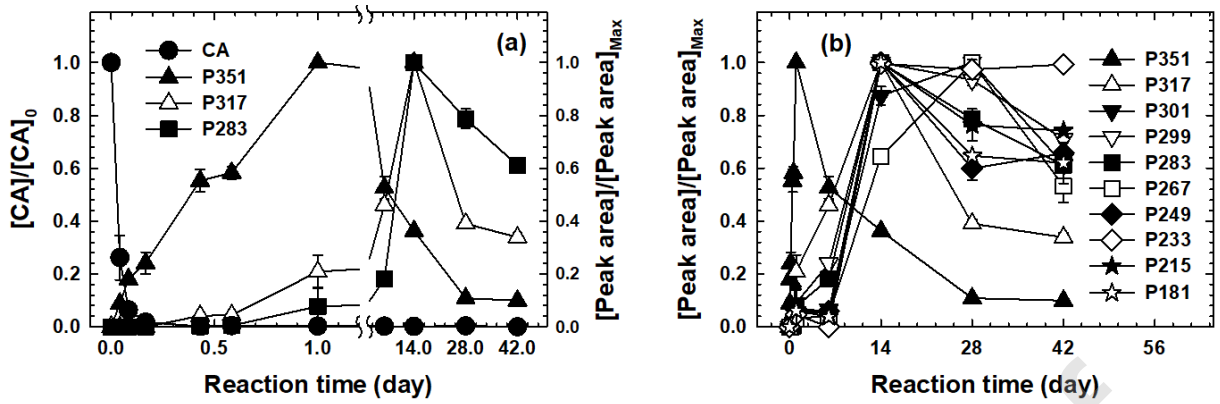

Fig. 2. Concentration-time profile of CA (a) and mass peak area-time profiles of the products (b). $[CA]_0$ = 0.1 mM, [ZVI] = 500 g/L, [MES] = 5 mM, $pH_{initial}$ = 7, pH_{final} = 7.54.

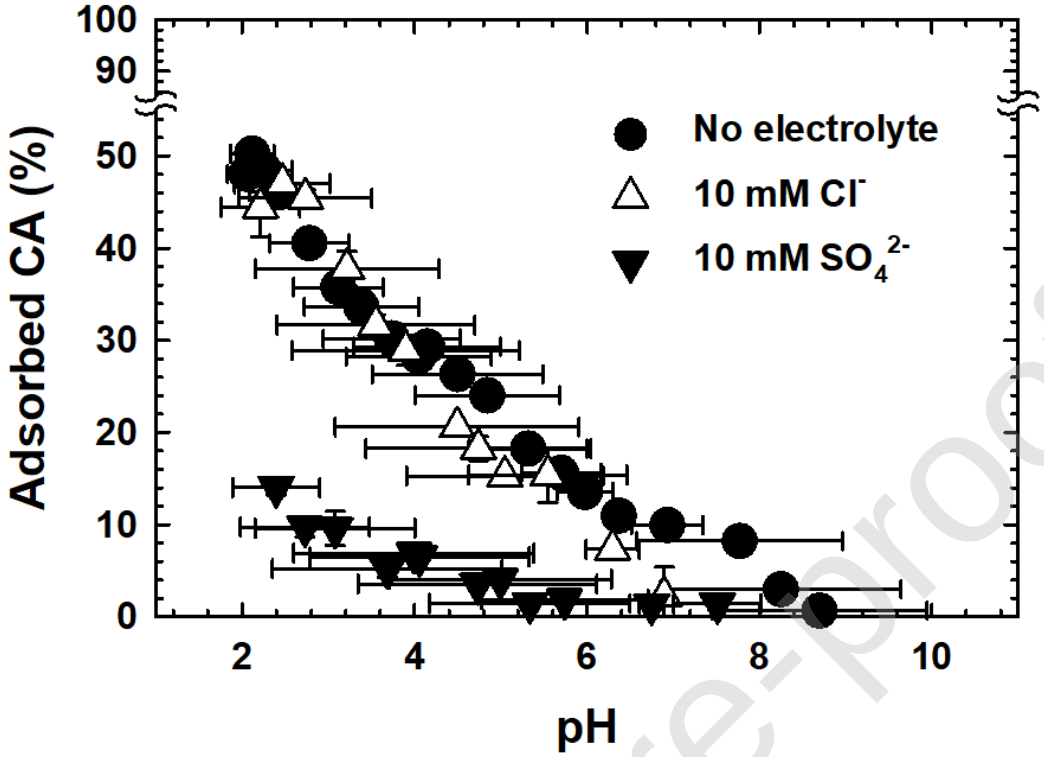

Fig. 3. Effect of pH on the adsorption of CA by ZVI. $[CA]_0$ = 0.1 mM, [ZVI] = 500 g/L. The contact time between CA and ZVI was less than 30 s. The solution pH was adjusted by H_2SO_4 or NaOH, and the solution did not contain any pH buffer.

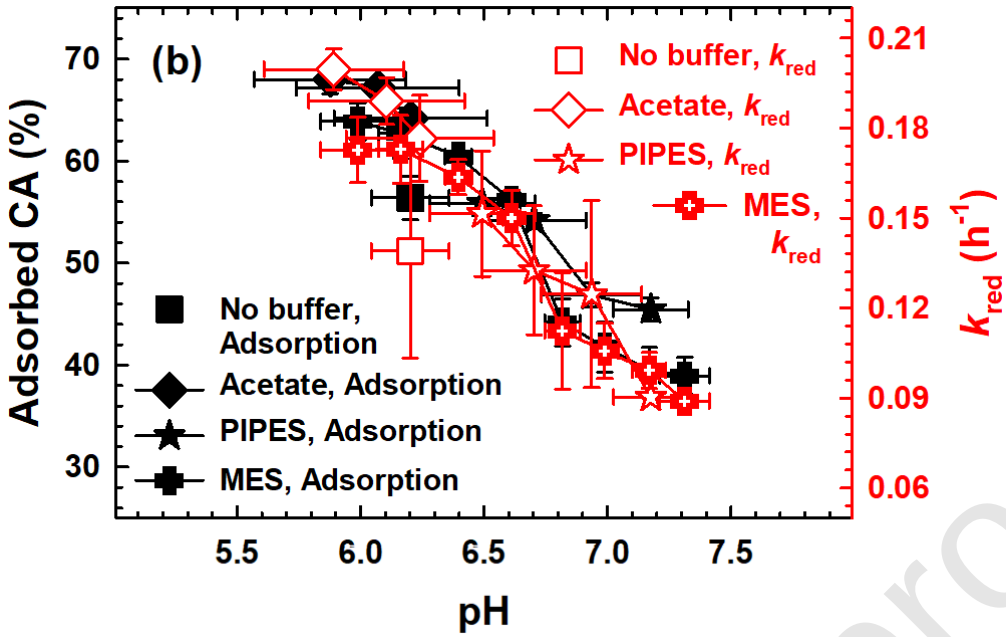

Fig. 4. Effect on pH on CA adsorption and degradation by ZVI. $[CA]_0$ = 0.1 mM, [ZVI] = 500 g/L. The solution pH was buffered by 5 mM of either MES, PIPES, or acetate.

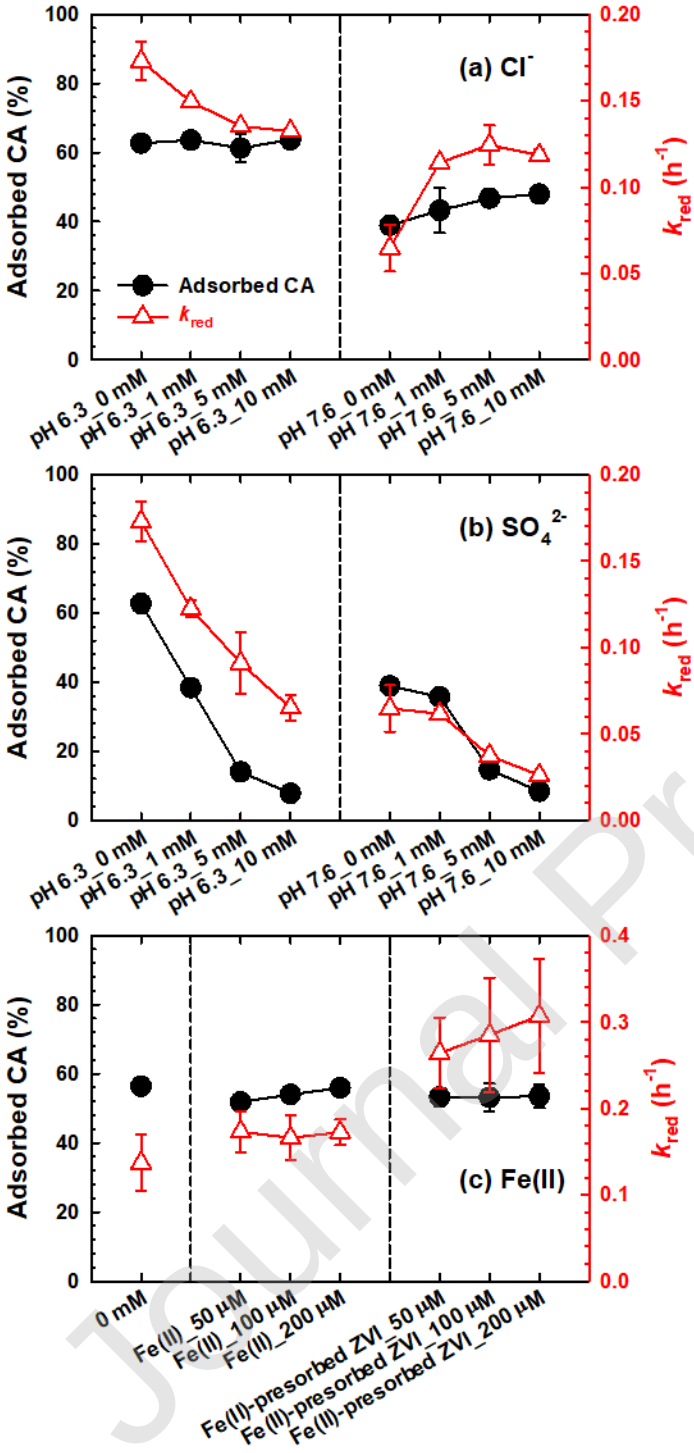

Fig. 5. Effects of (a) Cl^-, (b) SO_4^{2-}, and (c) Fe(II) on CA adsorption and degradation by ZVI. $[CA]_0$ = 0.1 mM, [ZVI] = 500 g/L, (a, b) [MES buffer] = 5 mM, (c) no buffer; pH_{ave} = 6.2.

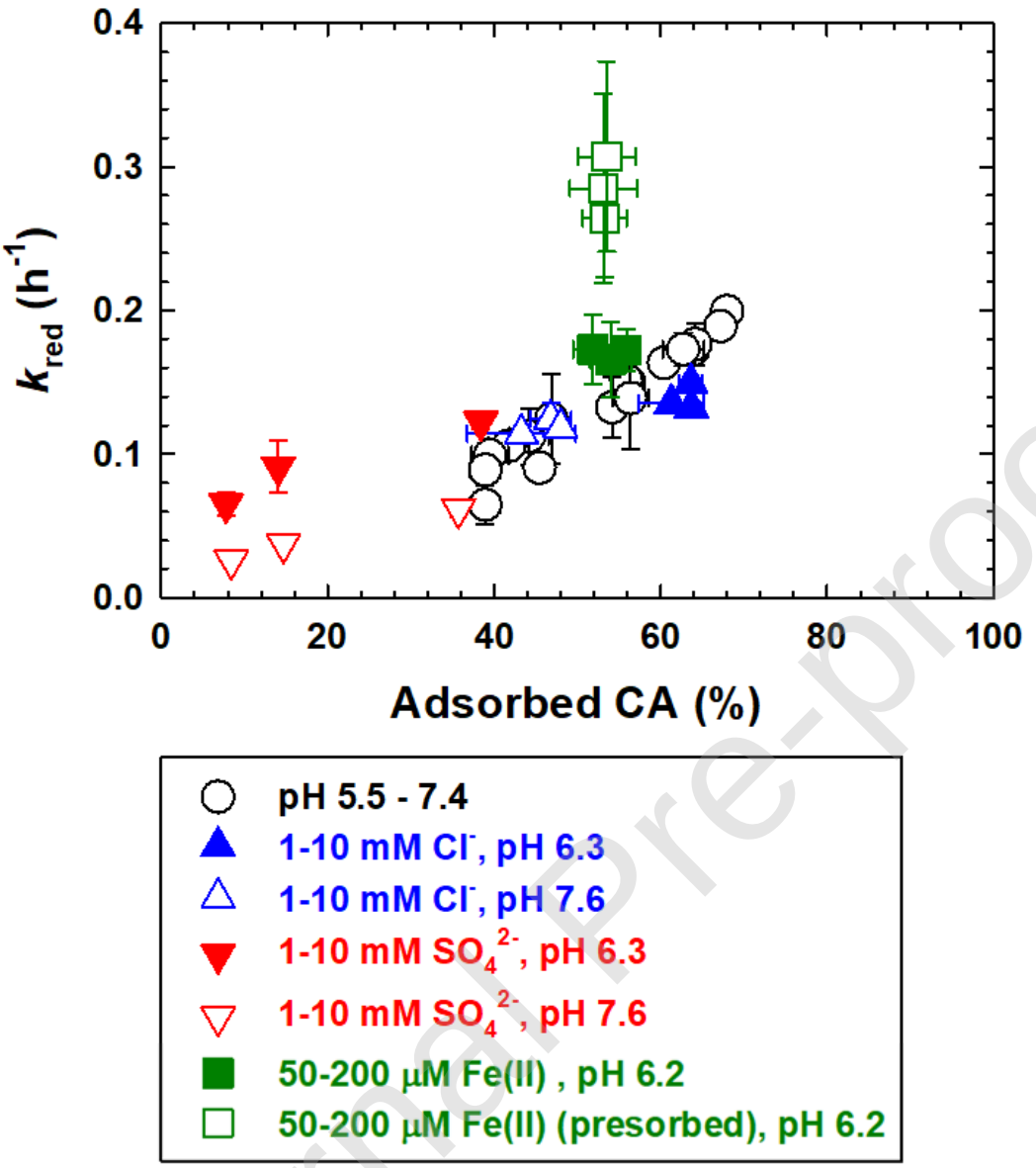

Fig. 6. Relationship between k_{red} and fraction of CA adsorbed on ZVI. All data were taken from Figure 4 and 5.